An Efficient Reactive Power Dispatch Method for Hybrid Photovoltaic and Superconducting Magnetic Energy Storage Inverters in Utility Grids

SAYED M. SAID[1,2]**, MOKHTAR ALY**[2,3]**, (Member, IEEE),**
AND HARTMANN BALINT[1]**, (Member, IEEE)**
[1]Department of Electric Power Engineering, Faculty of Electrical Engineering and Informatics, Budapest University of Technology and Economics, 1111 Budapest, Hungary
[2]Department of Electrical Engineering, Aswan University, Aswan 81542, Egypt
[3]Electronics Engineering Department, Universidad Tecnica Federico Santa Maria, Valparaiso 2390123, Chile

Corresponding author: Sayed M. Said (sayed.said@vet.bme.hu)

ABSTRACT The intermittent property and increased grid restrictions have become the most critical elements for increasing penetration levels of clean renewable energy sources (RESs). Smart inverters with combined RESs integration and reactive power support for utility grids have recently found widespread applications due to their techno-economic benefits. In smart inverters, the distribution-static compensator (DSTATCOM) functionality is inherently integrated to the RESs inverters. However, optimized reactive power-sharing between these inverters has become a big issue for the control systems of utility grids. There are numerous existing attempts presented in the literature for addressing these challenges, although they disadvantage low efficiency, uneven sharing, complex implementations, and/or costly added devices. Therefore, this paper proposes an efficient reactive power dispatch method between hybrid renewable energy generation and energy storage systems. The proposed method enhances the energy efficiency of the utility grid by adopting the reactive power share between interfacing inverters according to the estimated power losses. Besides, the proposed method enhances the reliability of smart inverters by relieving their thermal stresses through adopting their reactive power share according to the estimated power losses. The hybrid photovoltaic (PV) generation with superconducting magnetic energy storage (SMES) systems is selected as a case study for validating the new proposed reactive power dispatch method. The results, comprehensive discussions, and performance comparisons have verified the superior performance of the new proposed reactive power dispatch method.

INDEX TERMS Distribution static compensator, photovoltaic (PV), reactive power dispatch, smart inverters, superconducting magnetic energy storage (SMES).

I. INTRODUCTION

Ambitious installation plans of large scale photovoltaic (PV) power generation system have been targeted world-widely. The PV power generation systems have proven themselves as substitute candidates for replacing conventional fossil fuel-based generation systems. Being available everywhere, new and renewable, environmentally friendly, and having continuously reduced production cost represent the main advantages behind these ambitious plans [1], [2]. However, the fluctuated nature of PV generation systems during the day-time

The associate editor coordinating the review of this manuscript and approving it for publication was Reinaldo Tonkoski.

in addition to unavailability at night-time have given rise to energy storage systems (ESSs) installations for ensuring reliable power supply. In addition, grid restrictions have been imposed on PV systems operation to participate like the traditional generation systems, regarding the reactive power supply and support at various grid faults. Therefore, increased levels of PV penetrations in utility grids and their integrated ESSs have put reliability, energy efficiency, control of the power electronic interfacing converters of the prime concerns for both industry and research [3], [4].

The output power of PV systems is usually fluctuating during the day-time due to its dependency on the solar irradiance and ambient temperature [5], [6]. The ESSs are installed with

the PV systems to ensure reliable power supply, regardless of the output power of the PV systems. Thence, smoothing of the output power without fluctuations can be achieved [7], [8]. Several ESS technologies have been applied in the literature for PV systems. The superconducting magnetic energy storage (SMES) system has found wide applications as emerging technology due to its inherent advantages of high power density, fast response, high energy efficiency, and being environmentally friendly ESS [9].

The power electronic converters represent the principal element in proper utilization and energy transfer in PV generation and ESSs [10]. The fluctuated nature of the energy supply in the power converters results in improper optimized utilization of the power electronic capacities due to their design for the maximum operating point [11]. In addition, employing additional power converters for reactive power supply is usually employed in the power system for stabilizing and power factor improvement of the power systems. Recently, multi-functional power conversion systems have found wide application for PV and ESS integrated power systems [12]. The concept of smart power inverters has been introduced for power inverters with additional functionalities in utility grids. The smart inverter employs the oversized and/or the remaining capacity for performing the distribution static compensator (DSTATCOM) functionality [13], [14]. The PV-DSTATCOM and ESS-DSTATCOM are referred to grid interfacing inverters with dual functionalities of DSTATCOM in addition to PV and/or ESS integration, respectively. The added functionalities would result in increased power losses, which result in decreased reliability and operating lifetime of the inverter [15]. Therefore, research concerns have been risen for proper optimization of operating point and required functionalities of smart inverters for the control systems of utility grids.

The lack of reactive power dispatch increases the system active power loss, in addition to affecting the voltage profile and/or stability. In addition, it can make the system operates far away from the secure operating point. Several studies in the literature have discussed the reactive power dispatch issues. The application of optimization techniques for solving the reactive power dispatch issue in power systems is highlighted in [16]. Authors in [17] have proposed an optimal economic dispatch for combined heat and power units, intermittent energy sources, such as solar PV and wind, and battery energy storage system for balancing power and heat demand in power systems. In this study, hybrid particle swarm optimization (PSO) and sequential quadratic programming (SQP) method was applied for providing the optimal power produced from each energy source. A hybrid optimization approach has been presented in [18] through using the PSO method and the Tabu-search technique. This method can solve the reactive power dispatch problem for minimizing the line active power loss and the load bus voltage deviations. However, this method does not consider the fluctuating nature of renewable energy resources. In addition, the impacts of energy storage systems have not been studied in this method.

In [19], a two-level hierarchical control method is investigated to coordinate the reactive power dispatch in the clustered wind farms, which are located far away from each other with restriction in communications requirements. The coordinated control of voltage source inverters (VSIs) of the distributed generation (DG) units fed from different renewable energy sources was studied in [20]. The compensation of reactive power is shared without affecting the active power export. This in turn can improve the low-voltage ride through (LVRT) capability, and it can guarantee the seamless transition between LVRT and normal mode of operation. In [21], an approach using an evolutionary algorithm to find the optimal settings of the controllable components in the distribution system has been proposed. This method is capable of minimizing the system losses, the variations of voltage regulators and switching capacitors, and the active power curtailment of the PV system. This proposed method considers the impact of PV reactive power support to the grid in addition to the effect of high PV penetration on switching devices.

Authors in [22] have introduced the SMES device and its controllability to mitigate the stability of the utility power grid integrated with wind power generation. The connection of SMES at different locations is studied to suppress the power fluctuations and to improve LVRT performance. However, this study has not included the reduction of line power loss and the optimal calculation of SMES capacity to minimize the tie-line power flow. Authors in [23] have proposed a smart photovoltaic- distribution static compensator (PV-DSTATCOM) control method. The presented controller is capable of improving the power system quality and supporting the grid by supplying power to the grid and the connected loads. A similar controller of wind-DSTATCOM was presented in [13] with studying the impacts of the reactive power support and resilient microgrids operation of the inverter lifetime. The use of SMES devices for both grid-connected and islanded modes of operation for local load supplying and active/reactive power control was presented in [24].

It has become clear that the previously introduced control methods in the literature fail at addressing the challenge of smart inverters and efficient multi-functionalities operations of power converters. The current existing solutions possess the disadvantages of low operating efficiency, uneven sharing between the converters, complex control implementations, and requirements of costly devices. Therefore, induced by the aforementioned drawbacks of the existing control methods in the literature, this paper proposes an efficient reactive power dispatch between hybrid renewable energy generation and energy storage systems. The main contributions in this paper are summarized as the following:

- A new method for efficient operation for power systems with reactive power dispatch is presented.
- A cooperative reactive power sharing control method for PV-STATCOM and SMES-STATCOM inverters is proposed. The control of smart inverters with multi-functionalities is generalized in this paper.

- Thermal stresses reduction of power switches and hence reliability enhancement of smart power inverters methodology has been achieved using the new proposed method.
- Minimization of total power loss of the power inverter switches for both PV and SMES is investigated.

The remaining of the paper is organized according to the following items: Section II presents the modeling of the PV and SMES systems. The operation of smart inverters and the multilevel inverter are presented in Section III. The proposed control method and its implementation are detailed in Section IV. Section V gives the verification results and discussions of the new proposed system with the selected case study, in addition to the performance comparisons with the relevant techniques in the literature. Finally, Section VI presents the paper conclusion.

II. PV AND SMES SYSTEM MODELLING

Due to the critical necessity of the reactive power to provide loads and regulate the voltage profiles of buses, numerous challenges have been facing the grid-connected PV and energy storage system. These challenges are related to either grid issues and/or inverter issues. The grid side issues are due to the absorption of large reactive power from the grid would lead to increasing the transmission line power losses. This in turn results in minimizing the power system efficiency during the operation, especially at poor power factor loads. The inverter issues are related to the additional thermal stresses of their power semiconductor switches due to the injection of the reactive power into the utility grid.

A simplified representation of microgrid with PV power generation systems, SMES device for energy storage, and local power loads are shown in Fig. 1. The low voltage of the PV and SMES systems are connected to the point of common coupling (PCC) through stepping up transformers. The active power of the local loads are mostly powered from the PV, SMES, and grid according to the available and requested active power. Moreover, the local loads are mostly inductive loads with a low power factor (PF), and the reactive power supply can be achieved through the local inverters instead of absorption from the utility grid with more transmission line losses.

A. PV MODELLING

The single diode model of PV systems has been widely employed in the literature [25]. Fig. 2 shows the circuit equivalent electrical model of the single diode-based PV cell model. The generated output current of the PV cell I_{PV} can be modeled mathematically according to Fig. 2 as following [25]:

$$I_{PV} = I_{ph} - I_d - I_{sh} \tag{1}$$

The generated PV current can be modeled as follows:

$$I_{PV} = I_{ph} - I_s[\exp(\frac{V_{PV} + I_{PV}R_s}{aV_{tn}}) - 1] - \frac{V_{PV} + I_{PV}R_s}{R_{sh}} \tag{2}$$
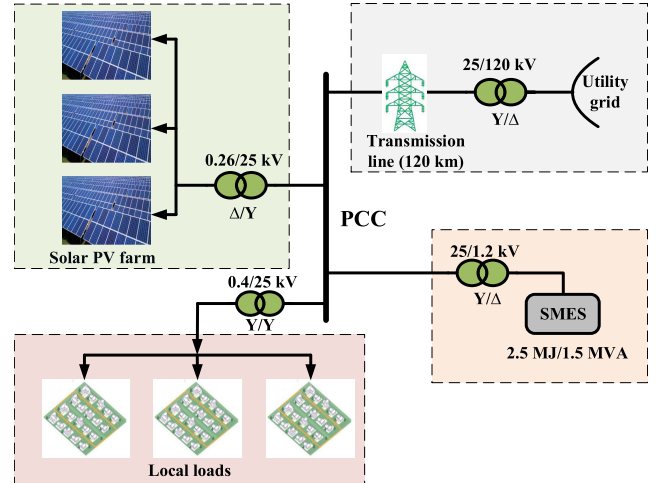

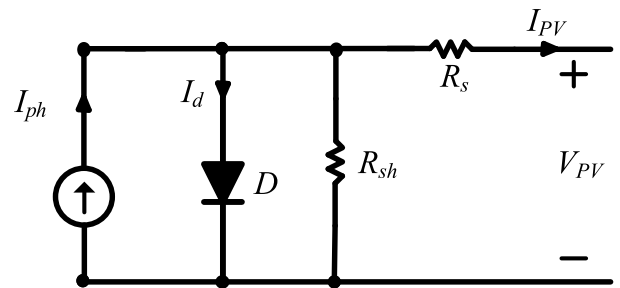**FIGURE 1.** Simplified microgrid structure with PV, SMES, loads at the PCC.

FIGURE 2. The electrical equivalent model of PV cells.

$$I_{ph} = I_{ph,n}(k_1(T_m - T_n))(\frac{G}{G_n}) \tag{3}$$

where I_s denotes the reverse saturation current of the diode. The parameters $I_{ph,n}$, V_{tn}, G_n represent the nominal datasheet parameters of photocurrent, the thermal voltage, and the solar PV irradiance, respectively. Whereas, the parameter k_1 denotes to the PV cell temperature coefficient at short-circuit current. In addition, the parameters T_m, and T_n represent the PV cell temperature (measured in °C), and the nominal PV temperature (normally at 25 °C), respectively.

B. SMES MODELLING

The operation of the SMES technology is through storing the electrical energy in the magnetic energy form. It is mainly composed of large superconducting inductance, which operates under the critical temperature to be preserved in its superconductor state. Fig. 3 shows the main constructing components of the SMES system. The system includes bidirectional dc/dc converter, bidirectional dc/ac inverter, SMES cooling system, and the coupling transformer. The bidirectional dc/dc converter is responsible for controlling the operating charging/standby/discharging mode of the SMES. In addition, the bidirectional dc/ac inverter controls the flow of the active and reactive power between the SMES system and the grid. The stored SMES energy E_{sm} is related to the
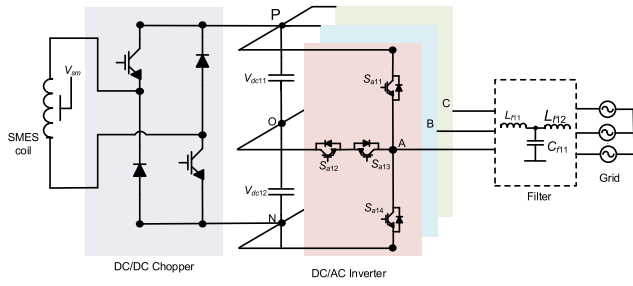
FIGURE 3. The main elements and structure of the SMES side.

TABLE 1. The power switches combinations for three-level T-type MLI.

Switching States	Switching signal ($x = a, b, c$)				Output Voltage
	S_{x21}	S_{x22}	S_{x23}	S_{x24}	V_{xo}
P-State	ON	ON	OFF	OFF	V_{dc21}
O-State	OFF	ON	ON	OFF	0
N-State	OFF	OFF	ON	ON	$-V_{dc22}$

SMES inductance L_{sm} and SMES current I_{sm} as following:

$$E_{sm} = 0.5 \times L_{sm} \times I_{sm}^2 \qquad (4)$$

whereas, the SMES active power P_{SMES}, the SMES voltage V_{sm}, the dc-link voltage V_{dc}, and the duty cycle D_m of dc/dc converter are related as the following:

$$P_{SMES} = V_{sm} \times I_{sm} \qquad (5)$$

$$V_{dc} = \frac{V_{sm}}{(2D_m - 1)} \qquad (6)$$

III. MULTILEVEL VOLTAGE SOURCE INVERTER MODELLING

Recently, the multilevel inverter (MLI) topologies have found vast attention by the researches in large-scale renewable energy applications due to their outstanding performance. The MLIs synthesize multilevel waveforms with high quality of injected grid currents without bulky low-frequency transformers. Among MLI topologies, the NPC-based MLI topologies have proved attractive practical applications in several industrial systems, especially in PV systems. NPC topologies eliminate the need for isolated dc sources in CHB topologies. Moreover, they eliminate the needed flying capacitors compared to the other existing topologies.

A. CIRCUIT TOPOLOGY

The T-type version of NPC topologies has been developed for improving their energy efficiency. The three-level T-type inverter combines the advantages of low switching power losses as in three-level MLIs and the low conduction power losses as in two-level inverters. The circuit topology of the three-level T-type inverter for grid-ties PV applications is shown in Fig. 4 [4]. The outputted voltage of each phase has three possible switching (namely *P* for positive, *O* for zero, and *N* for negative output voltages). The switching combinations of power switches for the T-type leg are shown in Table 1.
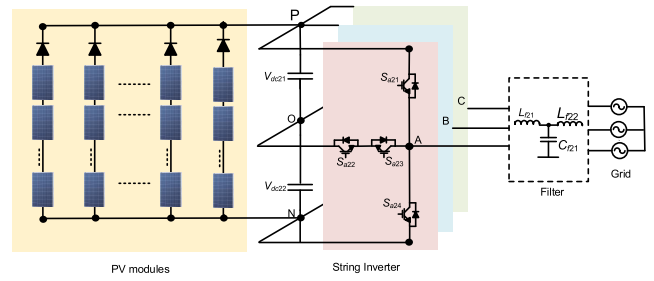

FIGURE 4. Grid-tied PV systems using the three-level T-type string inverter.

B. MODULATION METHOD

The voltage levels of the T-type inverter are generated through the modulation of the inverter. The level shifted pulse width modulation (LS-PWM) method is widely employed for T-type MLIs. The main waveforms for the LS-PWM method for a three-level T-type inverter and the corresponding switch gating signals are shown in Fig. 5. In the LS-PWM method, there are $(n - 1)$ requires carriers for the n number of output voltage levels of the inverter. The modulating signal and carriers for a three-level T-type inverter are shown in Fig. 5a. A continuous comparison during the switching period T_s of the modulating sinusoidal signal V_{mx} with the multilevel carriers. Then, the logic gates are employed for the generated output of the comparator to generate the switching gate pulses of the switches. The outputted voltage of the inverter and the filtered inverter current are shown in Fig. 5b. Whereas, the gating pulses for the power semiconductor switches in phase leg are shown in Fig. 5c.

C. CONTROL METHOD

The bidirectional voltage source converter (VSC) represent the main element for integrating the PV and SMES system to the utility grid. The controller for the grid-connected inverters at the PV generation and the SMES system are implemented using the d-q stationary reference frame control method [13]. Fig. 6a and Fig. 6b show the control schematic diagram of the PV and SMES inverters, respectively. The d-q reference frame controller for both systems is shown in Fig. 6c. There are two main functions of the bidirectional VSC in these systems, including the grid synchronization of the inverter system in addition to controlling the active/reactive power flow from or to the utility grid. In the proposed controller, the grid synchronization is performed through employing the phase-locked-loop (PLL) system [26]. The angle θ is extracted from the PLL system in order to perform the synchronization process. Detailed modeling and design of the controller with the system parameters can be found in [27], [28].

There are two bidirectional VSCs in the selected case study for integrating the PV system and SMES system to the utility grid. In both systems, the controller has to track properly the reference active power and reactive power for the inverter. For the PV system, the widely employed incremental
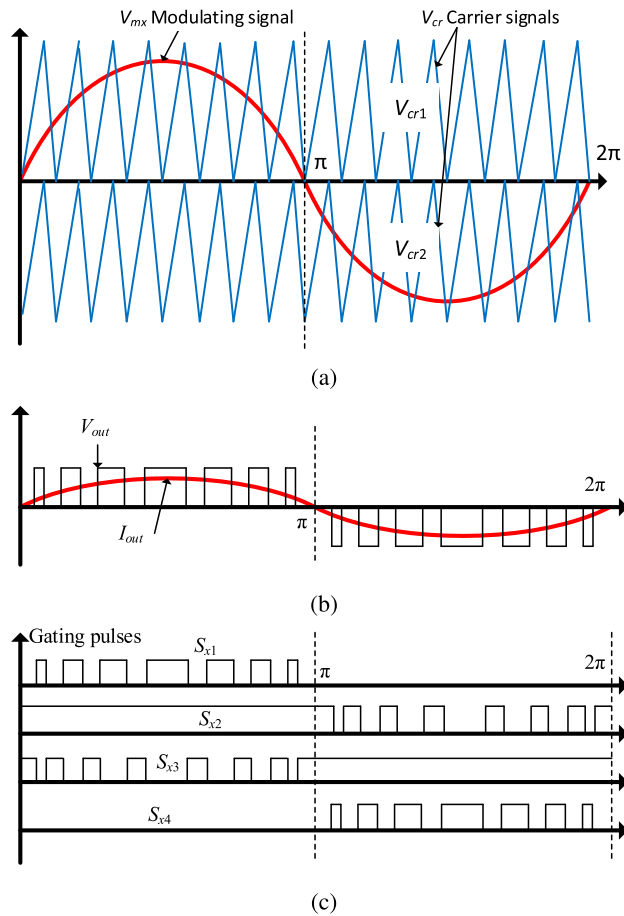
FIGURE 5. The operation of LS-PWM for three-level T-type inverter: (a) Modulating and carrier signals, (b) Outputted phase voltage and filtered current, and (c) Gating pulses of switches.

FIGURE 6. The control system of the VSCs at: (a) PV side controller, (b) SMES side controller, and (c) d-q controller structure.

conductance (INC) maximum power point tracking (MPPT) method is utilized. The sensed parameters of the PV array voltage V_{PV} and current I_{PV} are fed into the INC-MPPT method, which generates the duty cycle D_t of the PV side boost converter. Then, the reference active power $P_{PV,ref}$ is calculated using the measured parameters V_{PV} and I_{PV} of the PV system and fed into the d-q controller of the PV inverter system. Moreover, the design of the control system of SMES inverter is detailed in [3].

D. POWER LOSSES ANALYSIS
The employment of several VSCs in the hybrid system with different active/reactive power controls has made the estimations of the power losses of the converters of prime concern. The power losses modeling in this paper has been carried out in MATLAB based on numerical circuit simulations using the same basics in [29]. The power losses due to the operation of the three-level T-type inverter are analytically determined based on practical datasheet parameters from the manufacturer. The total power losses $P_{loss,switch}$ with the power switch can be calculated as follows:

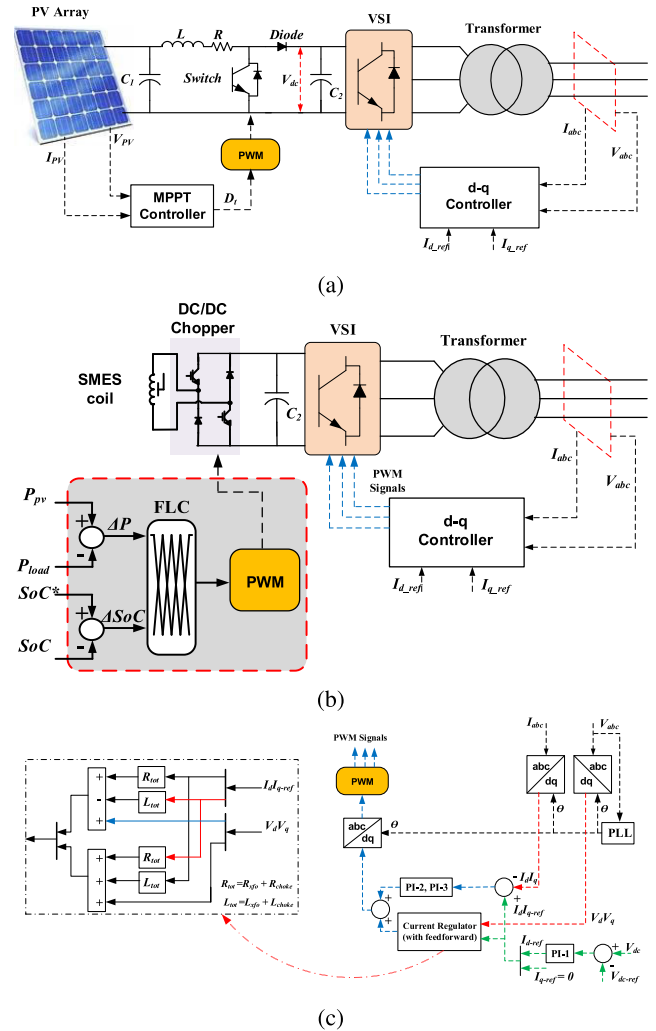$$P_{loss,switch} = P_{con,switch} + P_{sw,switch} \quad (7)$$

where $P_{con,switch}$ and $P_{sw,switch}$ denote to the conduction and switching power losses in the power switch. The switching power losses are composed of the turn on power losses $P_{on,switch}$ and the turn off power losses as following:

$$P_{sw,switch} = P_{on,switch} + P_{off,switch} \quad (8)$$

$$P_{sw,switch} = \frac{1}{t} \sum [E_{on}(I_{switch}, V_{switch}) + E_{off}(I_{switch}, V_{switch})] \quad (9)$$

where I_{switch} and V_{switch} are the forward current through the switch and the terminal voltage at any instant, respectively. The parameters E_{on} and E_{off} represent the turn on and turn off energy of the switch, and they are normally given in the manufacturer datasheet. Whereas, t denotes the time period for the estimated switch loss. The power losses are calculated based on the instantaneous measured switch voltage and current. The conduction power losses $P_{con,switch}$ of the switch, the turn on power losses $P_{on,switch}$ for one transition and the turn off power losses $P_{off,switch}$ for one transition are calculated as

follows:

$$P_{con,switch} = I_{switch}V_{f,switch}) + I_{switch}^2 R_{switch} \tag{10}$$

$$P_{on,switch} = E_{on}\frac{I_{switch}V_{switch,pre}}{I_{switch,ref}V_{switch,ref}}\frac{1}{\Delta t} \tag{11}$$

$$P_{off,switch} = E_{off}\frac{I_{switch,pre}V_{switch}}{I_{switch,ref}V_{switch,ref}}\frac{1}{\Delta t} \tag{12}$$

where $V_{f,switch}$, and R_{switch} represent the forward voltage and on resistance of the switch. $I_{switch,pre}$ and $V_{switch,pre}$ are delayed one instant measured current I_{switch} and voltage V_{switch} of the switch, respectively. The parameters $I_{switch,ref}$ and $V_{switch,ref}$ denote to the reference current and voltage from manufacturer datasheet in the switching energies calculation tests. The parameter δt denotes to the simulation time step of the MATLAB.

In the instantaneous power losses estimations, it is crucial to define the turning on and off instants of the power switch. For the power switch, the detection of the switch turn on status (Turn on when ($I_{switch,pre} = 0$) and ($V_{switch,pre} > V_{f,switch} + I_{switch,pre}R_{switch}$) and ($I_{switch} > 0$)). Whereas the turn off status is detected (Turn off when ($I_{switch,pre} > 0$) and ($V_{switch} > V_{f,switch} + I_{switch}R_{switch}$) and ($I_{switch} = 0$)). The same analysis can be made for the power semiconductor diodes when the measured current of the switch is negative. The conduction power losses can be estimated using (10) and the parameters of the diode datasheet. Whereas, the switching power losses of the diode is calculated using (12) with replacing the turn off energy of the switch with the diode reverse recovery energy. The reverse recovery is detected using the diode current and voltage (Reverse recovery when ($I_{switch,pre} < 0$) and ($V_{diode} < V_{f,diode}$). Where V_{diode} and $V_{f,diode}$ denote to the measured diode voltage and forward voltage drop of the diode.

IV. THE PROPOSED REACTIVE POWER DISPATCH METHOD

In the new proposed method, a cooperative control strategy is applied between the two power inverters of PV and SMES systems to achieve the local optimized reactive power dispatch between the two inverters. Therefore, the PV and SMES converters supply the local load completely by minimizing the total power losses of power switches for the two inverters in accordance. This in turn can reduce the thermal stress of the switches compared to the conventional uncooperative reactive power control of the two inverters. The main objective of the new proposed method is to share the required load reactive power locally between the PV and SMES power inverters in order to achieve several objectives, which can be summarized as follows:

- Minimizing the active and reactive powers come from the utility grid as possible with achieving supply of the local load cooperatively among the PV and SMES inverters. While, the PCC voltage profile is regulated within the permissible limit in the grid codes for the whole day operation.

- Reducing the total power losses of the power switches in the PV and SMES inverters during all modes of operation.
- As a direct benefit of applying the proposed dispatch method, decreasing the thermal stresses of power switches compared to the uncooperative reactive power-sharing methods between the two power inverters.
- Enhancing the microgrid reliability during the intermittent PV power supply at integrated fixed and variable loads scenarios.

Fig. 7 shows the main elements of the power system and the proposed control structure. Each of the PV and SMES systems has its local d-q controller that regulates the measured currents to follow the reference currents. Whereas, the central controller of the two inverters using the new proposed algorithm manages the mode and amount of active and/or reactive power flow of the system. The main objectives of the system are to extract the maximum power point (MPPT) of the PV system, achieving local power supply of the load and accordingly minimizing the power from the utility grid. The generalized objective function of the active and reactive power supply to formulate the objectives in the new proposed method can be written as follows:

$$Minimize\ [\ Q_l - \sum(Q_{pv} + Q_{SMES})] \tag{13}$$

$$Minimize\ [\ P_l - \sum(P_{pv} + P_{SMES})] \tag{14}$$

The cooperative active and reactive power control is achieved in terms of load reactive power (Q_l), PV inverter's reactive power (Q_{pv}), reactive power of the SMES inverter (Q_{SMES}). Fig. 8 illustrates the complete flowchart of the proposed active and reactive power control method between PV and SMES inverters. There are two consecutive controllers for active and reactive power references of the two inverters. The main steps of the proposed active and reactive power sharing method can be summarized as follows:

Step 1: The system parameters are measured through the advanced metering infrastructures in the power systems. The parameters include the measurement of the load active and reactive power demand (P_l and Q_l), the extracted MPPT power pf the PV generation system (P_{pv}), and the available state of charge of the SMES system (SMES SoC).

Step 2: The active power flow is controlled by the PV and SMES inverters side and the utility grid side. The active power of the load demand (P_l) is compared to the extracted MPPT power from the PV (P_{pv}). When the PV power exceeds the demanded load power, the excess power is used for charging the SMES until the maximum SoC (SoC_{max}) is reached and then the excess power is injected to the utility grid. From another side, if the generated PV power is lower than the demanded load active power, the difference is covered by the SMES until the SoC of SMES reaches the minimum value (SoC_{min}). Then, the required power is absorbed from the grid when the PV and SMES active power do not fulfill the load requirements of the active power.
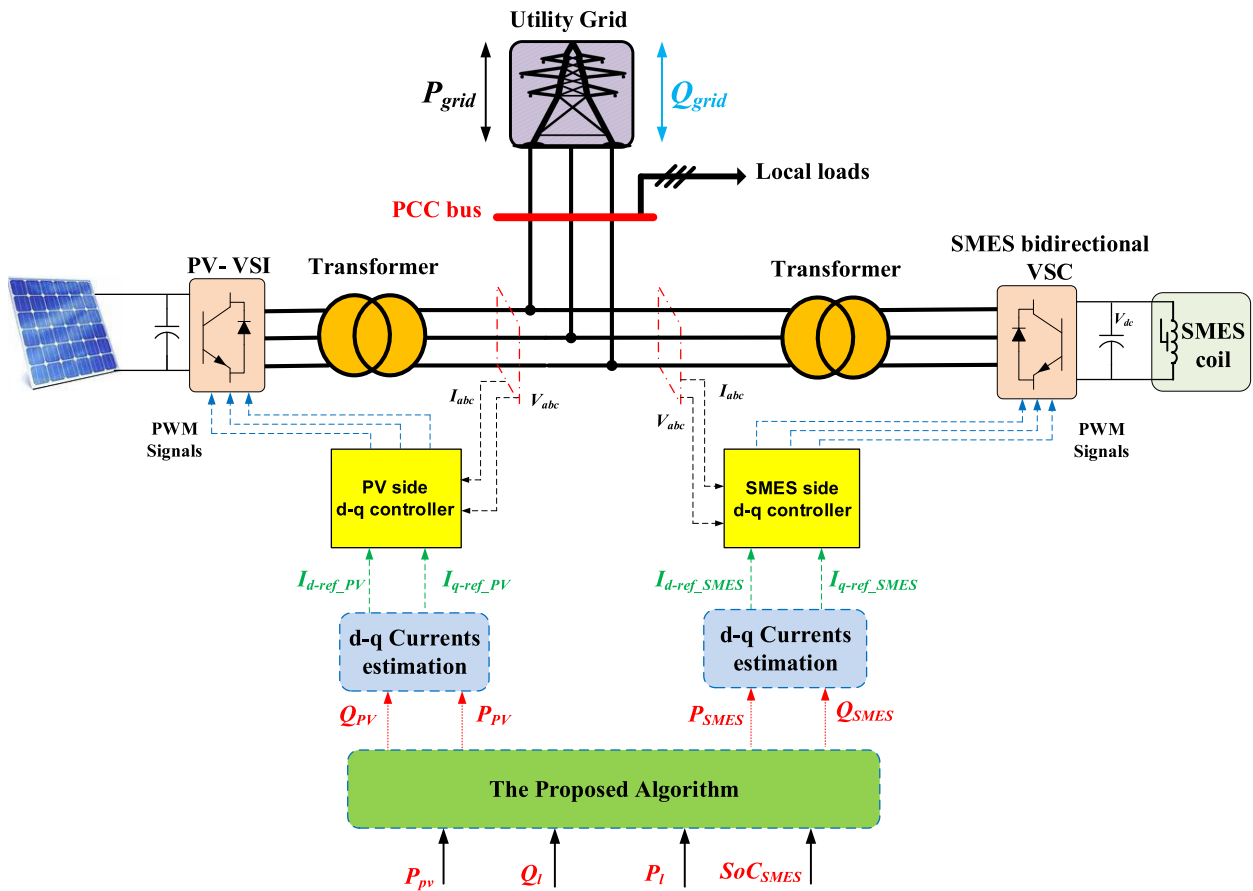
FIGURE 7. The power system structure and the new control method for hybrid PV and SMES power systems.

Step 3: Afterwards, the remaining available reactive power capability of the PV and SMES inverters are calculated through using the previously estimated active power and the known capacities of the inverters. In this step, the amount of available reactive power in the PV inverter Q_{a-pv} and the SMES inverter Q_{a-SMES} are determined for the reactive power sharing control. The available Q_{a-pv} and Q_{a-SMES} are calculated as the following:

$$Q_{a-pv} = \sqrt{S_{pv}^2 - P_{pv}^2} \qquad (15)$$

$$Q_{a-SMES} = \sqrt{S_{SMES}^2 - P_{SMES}^2} \qquad (16)$$

where S_{pv} and S_{SMES} represent the capacity of the PV inverter, and SMES inverter, respectively. The active power P_{pv} and P_{SMES} represent the MPPT generated power and the SMES charging/discharging power command as in step 2, respectively.

Step 4: The second stage is the control of reactive power sharing of the PV and SMES inverters. The available maximum reactive power share of each of the connected inverters are determined in step 3. A priority is given within the proposed approach to minimize the reactive power absorption/injection with the grid. Whereas, the local reactive power supply is achieved through the local PV and SMES inverters. In case of the required load reactive power is lower than

the sum of available reactive power capability of the PV and SMES inverter, the total demanded reactive power is shared by local PV and SMES inverters. The sharing can be symmetrical when both of the inverters can supply half of the required load reactive power. Whereas, the reactive power sharing can be asymmetrical in the case of the two inverters has available reactive power lower than the half of the required load reactive power. In this case, the reactive power sharing is controlled asymmetrically to fulfill the local load supply. From another side, the grid contributed to the reactive power supply in case of the required load reactive power exceeds the sum of the available reactive power in PV and SMES inverters. Lastly, the reference dq currents for the two inverters are obtained using the reference active and reactive power for each inverter [27]. Therefore, the local active and reactive power supply can be achieved using the new proposed algorithm, whereas, the absorbed active and reactive power from the grid is minimized. Thence, enhanced energy efficiency and reliability can be achieved by applying the new proposed method.

V. RESULTS AND DISCUSSIONS
The grid connected hybrid PV-SMES microgrid distribution system is used as a case study to verify the new reactive power dispatch method. Two scenarios are studied, the first one is
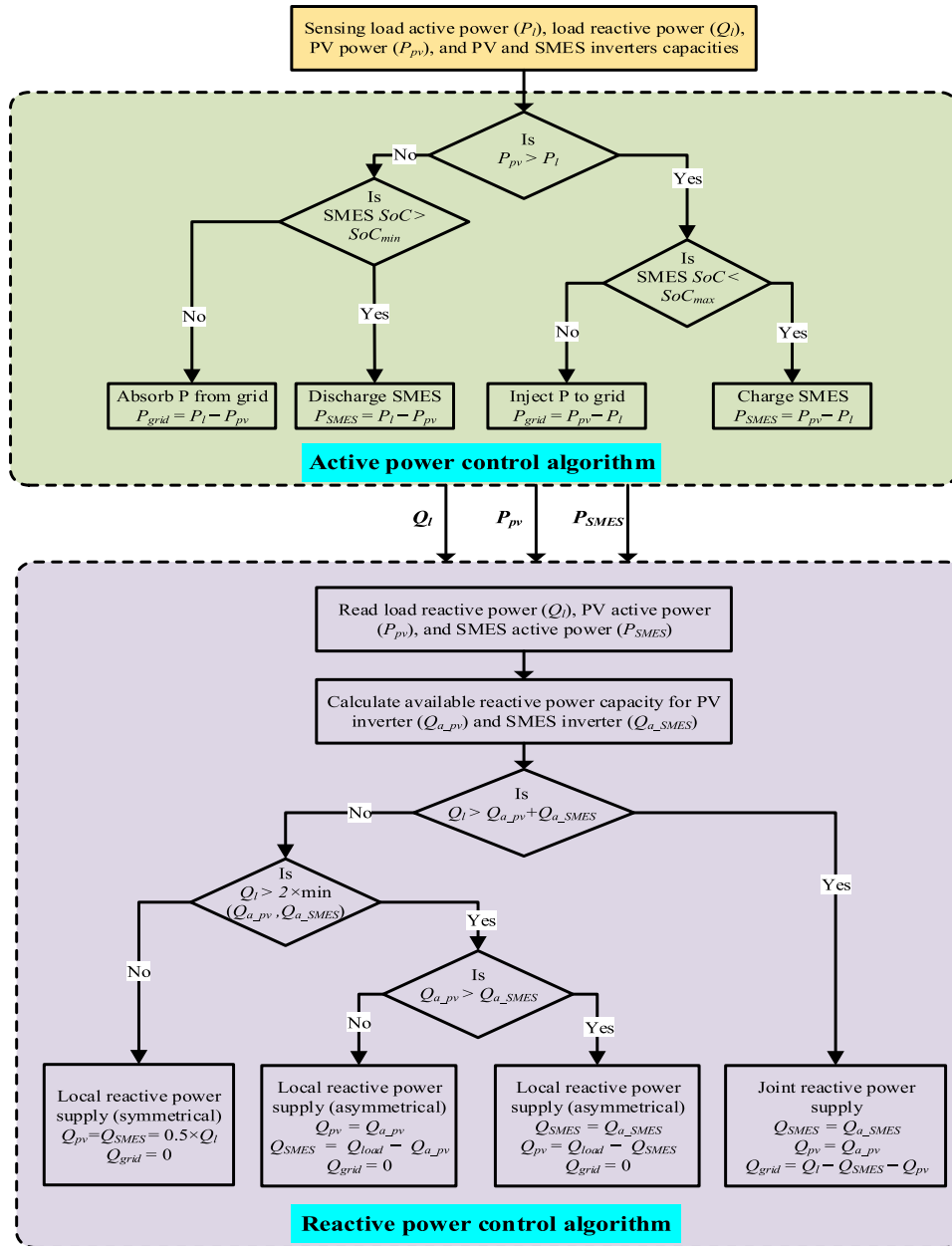
**FIGURE 8.** Flowchart of the proposed active and reactive power control method.

during a fixed load (250 kW, 0.707 lagging power factor) and the second scenario is at a variable load condition as shown in Fig. 1. The SMES has 1000 A, an initial current, 5 H coil inductance, and 1.5 MVA SMES VSC capacity. The detailed simulation parameters of the selected case study are given in [30]. The two scenarios have been tested with four cases, which can be summarized as follows:

- *Case 1:* PV only without injecting reactive power (i.e., $Q_{pv} = 0.0$),
- *Case 2:* PV only with injecting reactive power is equal to 50% of the load reactive power (i.e., $Q_{pv} = 50\%Q_l$),
- *Case 3:* PV only with injecting reactive power is equal to full load reactive power (i.e., $Q_{pv} = 100\%Q_l$),

- *Case 4:* PV and SMES with equally sharing of the injecting load reactive power (i.e., $Q_{pv} = 50\%Q_l$ and $Q_{SMES} = 50\%Q_l$).

A. FIXED LOADING SCENARIO

In this scenario, the abovementioned four cases are tested in the presence of a fixed load connected with the microgrid system. Fig. 9a shows the response of reactive power for the four tested cases as described above. It is clear that in case 4, the load reactive power is completely compensated with the cooperation between PV and SMES inverters equally and there is no reactive power absorbed from the utility grid. On the other hand, in cases 1, 2, and 3, reactive power is
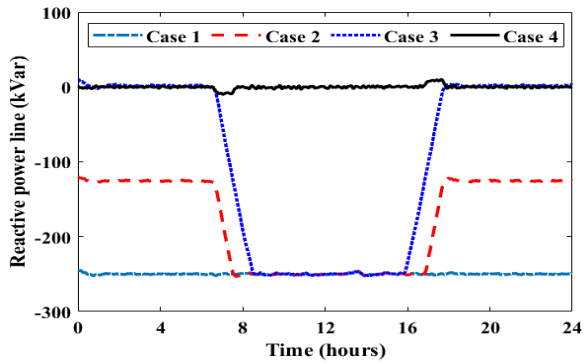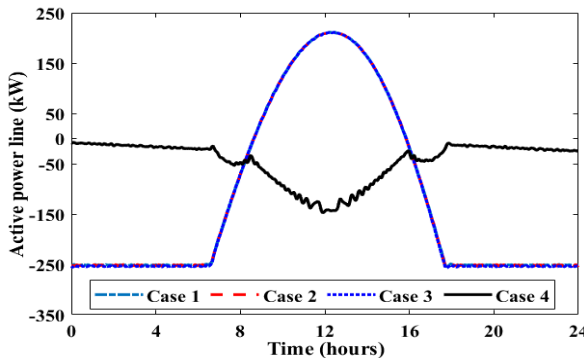
(a) The reactive power of line at the PCC.
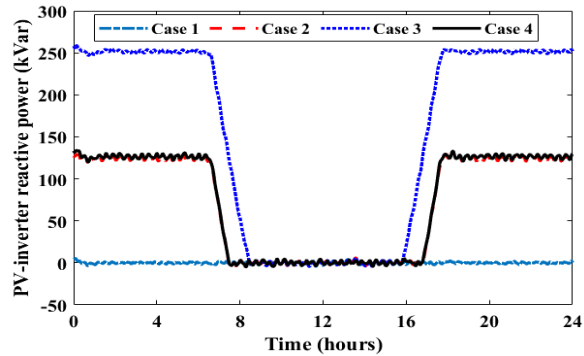
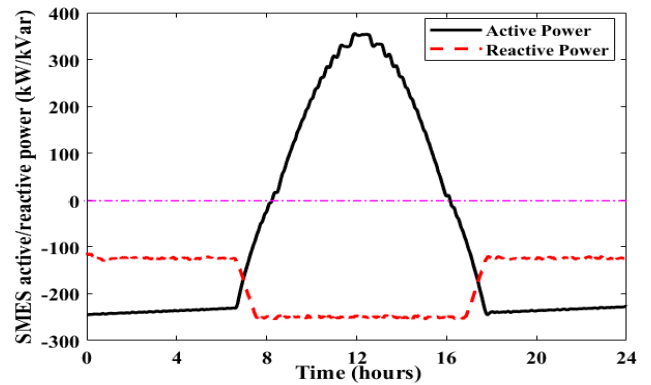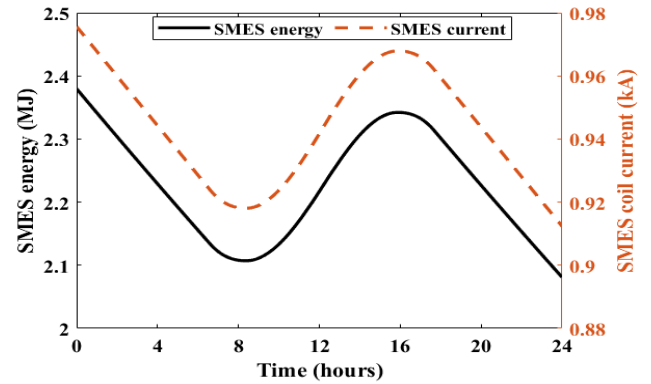(b) The reactive power of PV inverter.
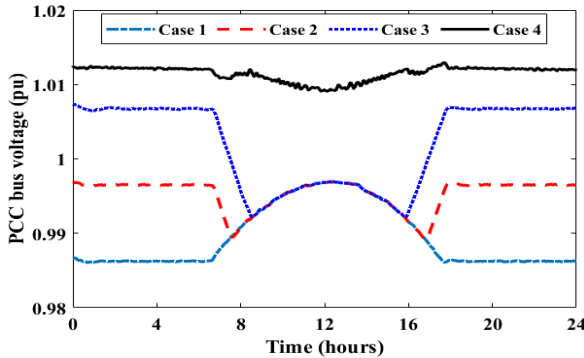
(c) The PCC voltage.

(d) The active power exchange with the line at PCC.

FIGURE 9. The daily profiles of the active and reactive power at a fixed load profile.

(a) Active and reactive power of SMES inverter.

(b) Current and stored energy of SMES coil.

(c) The dc-link voltage and voltage of SMES coil.

FIGURE 10. The performance of the SMES side power conversion system at a fixed load profile.

microgrid. In both cases 2 and 4, the PV inverter injects half of the load reactive power. Hence, it operates with lower thermal stresses than at case 3 because the output inverter's reactive power peak is 250 kVAR in case 2 and 4, and it is equal to 500 kVAR in case 3 during a period of no generation PV power. The PV inverter reactive power reduces by starting in a generation of the PV active power due to the inverter capacity limit. The injected reactive power reaches zero value at the period of the peak PV active power generation.

Fig. 9c shows the PCC voltage profile in four cases, it can be seen that the voltage profile is approximately constant at 1.01 p.u. during the whole day in the case of equally
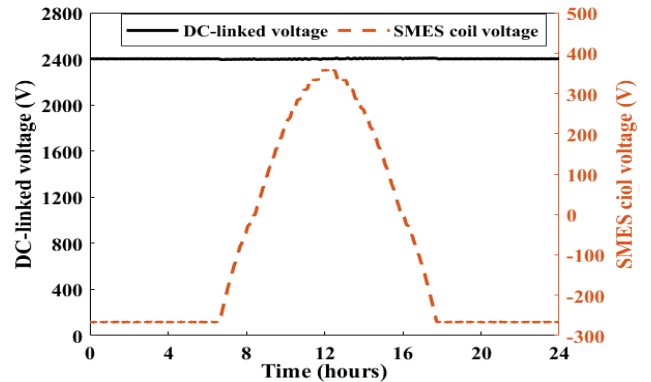
required to be absorbed from the grid to provide the load reactive power. The output reactive power of PV inverter is discussed in Fig. 9b for the four operating cases of the

load reactive power sharing between PV and SMES inverters. Case 1 represents the worst scenario regarding the PCC voltage profile due to the fluctuating power of PV generation and the absence of the SMES. Whereas, injecting local reactive power in cases 2, 3, and 4 helps at regulating the PCC voltage. It can be also seen that the difference among cases 2, and 3 with case 4 due to the incorporation of SMES with better voltage regulation for the whole daily profile. The behavior of line active power exchange with the utility grid at the PCC is shown in Fig. 9d. The utilization of SMES in case 4 achieves minimal absorbed active power from the grid at the PCC. In which, the SMES cooperates with PV in supplying the local load with active and reactive power demands. In addition, the absence of SMES and PV generation in the night time in the other cases requires power absorption from the grid.

The performance of the SMES and its power conversion are shown in Fig. 10. The active and reactive power of the SMES side power conversion system are shown in Fig. 10a. The stored SMES energy is transferred to the connected load during the absence and insufficient generation of the PV system. This, in turn, helps at providing local active power supply for the load in addition to smoothing the power generation of the fluctuated in nature PV system. Moreover, the reactive power is shared among the PV and SMES inverters during the night time. Whereas reactive power supply is made through the SMES inverter during peak PV generation due to the capacity of the PV inverter. Thence, the new proposed sharing strategy can provide local active and reactive power supply and hence reducing the dependency of powers come from the utility grid as possible.

From another side, the SMES coil current and its stored energy for the daily load profile are shown in Fig. 10b. It can be seen that both of them start from its initial state then it decreases during the discharge mode of SMES. Then, they increase during the charge mode of the SMES when the PV generation exceeds the load demand. It can be seen also the smooth current and energy transfer from/to the SMES coil using the proposed control strategy. Fig. 10c shows the dc-link voltage of the SMES inverter and the voltage of SMES coil. The voltage of dc-link capacitor is approximately constant at 2400 V during all modes of operation. In addition, the polarity of the voltage across the SMES coil is determined according to the required charge/discharge operation.

Fig. 11 provides the comparison of the daily inverter power losses of the PV and SMES inverters in cases 3 and case 4. It can be seen that great improvement is achieved in the total switching power loss with case 4 with applying the dispatchable reactive power method between PV and SMES inverters than in case 3. The average power losses for the inverters for case 3 is 2.457 kW, whereas the average power losses for case 4 is 1.826 kW. This, in turn, leads to a reduction of 25.7% of the power losses due to sharing the reactive power sharing between the SMES and PV inverter compared to supplying the reactive power by only the PV inverter.
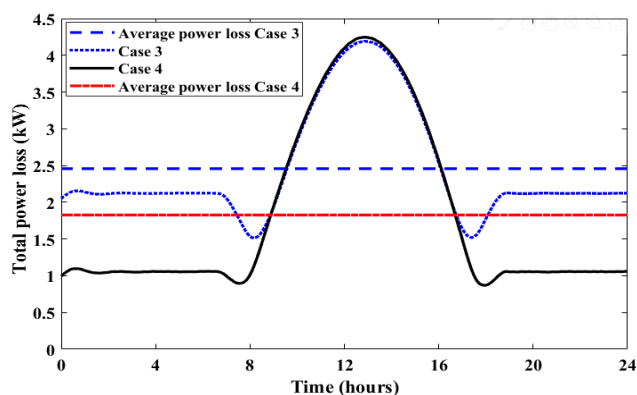

FIGURE 11. Comparison of the total power loss of PV and SMES inverters at case 3, and case 4 at fixed load scenario.
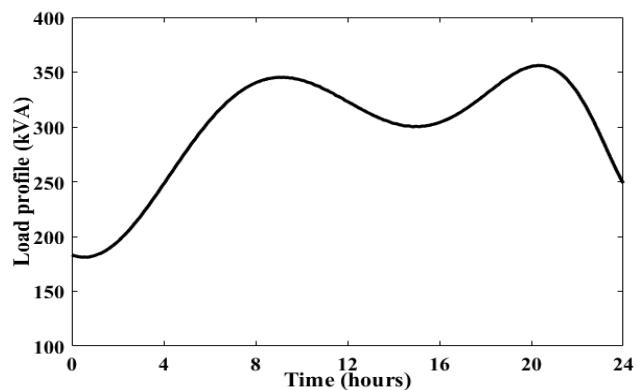

FIGURE 12. The daily profile for the variable load demand condition.

B. VARIABLE LOADING SCENARIO

Additionally, the proposed strategy is investigated using the case study of variable load, which is integrated into the grid connected hybrid PV-SMES microgrid distribution system. The loading profile for the selected case study is shown in Fig. 12. It is assumed that the power factor of the load is fixed at 0.707 lagging for the daily load demand. The system is tested for the same abovementioned four operating scenarios. The tested cases are analyzed to prove the effectiveness of the proposed dispatchable reactive power method.

The system performance for the variable load scenario is shown in Fig. 13. Fig. 13a shows the line reactive power at PCC in the presence of the variable load demand for the four cases. By applying the dispatch reactive power between PV and SMES, completely load reactive power supplying can be achieved locally from the sharing between PV and SMES inverters in case 4. Whereas, the contribution of the utility grid in injecting reactive power is needed in all other three cases (case 1, case 2, case 3) to provide the variable load especially the PV generation power period.

From another side, the reactive power supply by the PV inverter for the four cases is shown in Fig. 13b. The reactive power of the load demand is shared between the PV inverter and the utility grid in case 2. Whereas, it is shared between the PV inverter and the SMES inverter for case 4. This leads to lowering the thermal stresses of the inverter system,
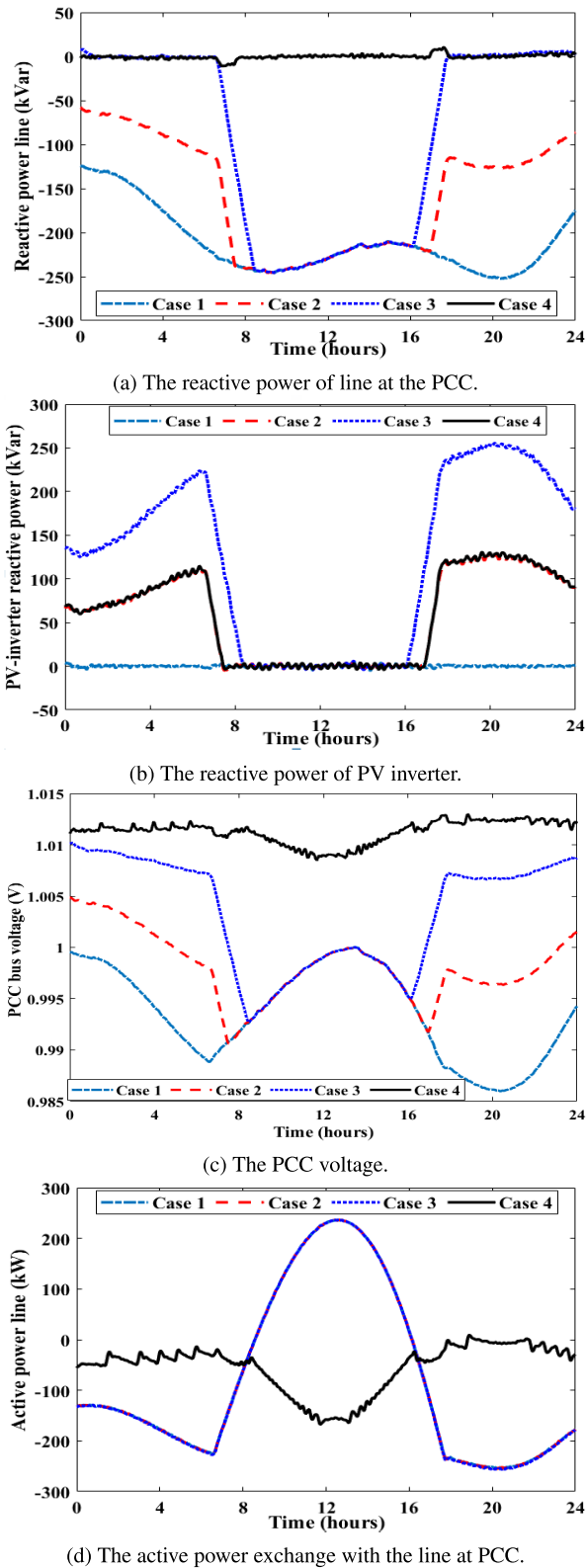
(a) The reactive power of line at the PCC.

(b) The reactive power of PV inverter.

(c) The PCC voltage.

(d) The active power exchange with the line at PCC.

FIGURE 13. The daily profiles of the active and reactive power at variable load profile.

which enables the PV inverter to perform its function with more flexibility. Moreover, a prolonged operating lifetime of the inverter can be achieved for case 2 and case 4 of the

PV inverter. The voltages at the PCC for the four cases are shown in Fig. 13c. It can be seen that the proposed sharing strategy preserves fixed voltage at PCC compared with the other cases.

The active power exchange at the PCC for the four cases with variable load demand is shown in Fig. 13d. It is clear that the minimum active power exchange with the utility grid is achieved using the proposed strategy in case 4. This is as a direct result of employing the SMES system for providing the suitable support of active power. The proposed method can help in enhancing the reliability of power supply and reducing the energy loss due to grid transmission of the active power. Whereas, the other cases require the utility grid for supplying the extra demanded energy and compensating the variability of the outputted power of the PV generation systems.
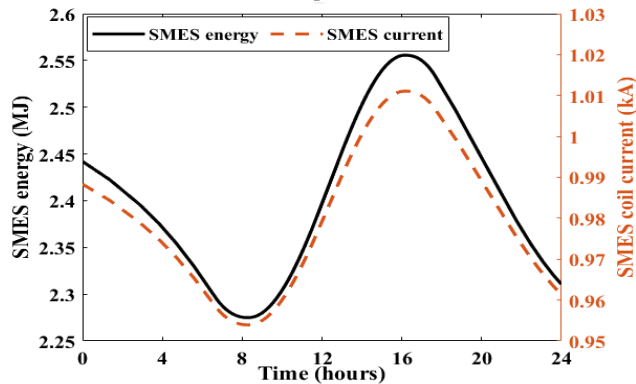
The performance of the SMES side power conversion systems is shown in Fig. 14. Fig. 14a shows the active and reactive power exchange of the SMES-side inverter for case 4. It can be seen that the SMES inverter supply the load active power during night time, whereas it absorbs the remaining power of the PV during the day time. Moreover, the SMES inverter shares the reactive power with the PV inverter during the absence of solar irradiance at night time. Whereas, the SMES inverter supply the reactive power required by the load during the PV generation peaks due to the limited capacity of the PV inverter.

The corresponding SMES current and energy for the variable load condition with case 4 are shown in Fig. 14b. It can be seen that the SMES current and energy are decreasing simultaneously during the discharging mode. Whereas, they are simultaneously increasing during the charging mode. A smooth power transfer from/to the SMES coil is achieved using the proposed control strategy. The performance of the dc-link voltage and the SMES coil voltage are shown in Fig. 14c. It is clear that the dc-link voltage is regulated to be fixed without fluctuations with the load variations. The control of the dc-link voltage is crucial for determining the operating lifetime and thermal stresses of the dc-link capacitors.

The total power losses of the SMES and PV inverter for case 3 and case 4 are compared in Fig. 15. The reactive power share between the two inverters in case 4 can help to reduce the total power losses than case 3. This, in turn, enhances the energy efficiency of the power conversion system in addition to reducing the stresses of the power electronic components of the inverters. In particular, the thermal stresses are proportionally related to the power losses in the inverter system. Therefore, reduced thermal stresses and longer lifetime are achieved through the proposed reactive power sharing strategy. The average power losses of the daily power losses are estimated for case 3 and case 4. The new proposed sharing strategy achieves average power losses of 1.696 kW, whereas case 3 has 2.179 kW average power losses. This, in turn, leads to about 22.2% improvement as a direct result of applying the new proposed reactive power sharing strategy. Moreover,
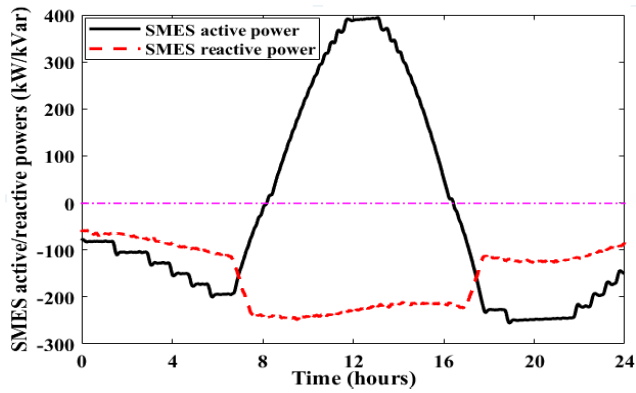
(a) Active and reactive power of SMES inverter.

(b) Current and stored energy of SMES coil.
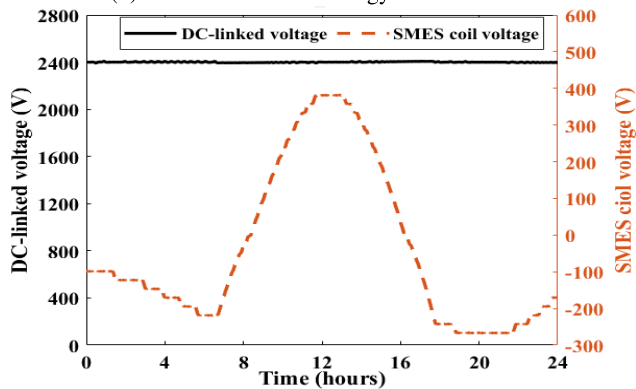
(c) The dc-link voltage and voltage of SMES coil.

FIGURE 14. The performance of the SMES side power conversion system at a variable load profile.

Fig. 16 shows the comparison of SMES AC power losses at fixed and variable load scenarios. The curve fitting method in [31] is used for the estimation of the AC power losses of the SMES device. It can be seen that the variable load scenario exhibits more AC power losses in the SMES device than the fixed load scenario. This is due to the required active power exchange at the variable load scenario.

C. PERFORMANCE COMPARISON

Table 2 summarizes the various performance metrics and comparisons of the various operating scenarios. The four scenarios include the existence of SMES system and the
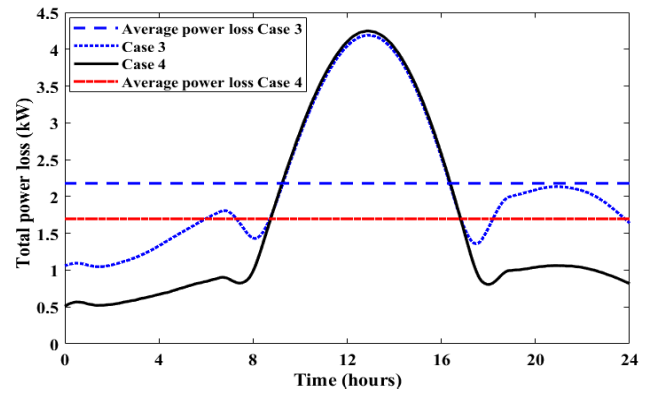

FIGURE 15. Comparison of the total power loss of PV and SMES inverters at case 3, and case 4 at variable load scenario.
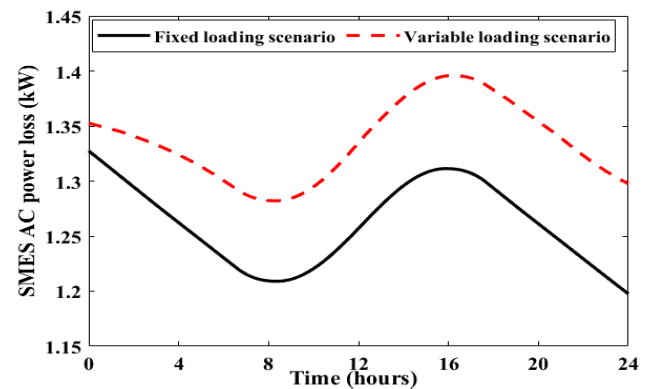

FIGURE 16. Comparison of the SMES power loss at fixed and variable load scenarios.

additional functionality of reactive power sharing by the SMES and PV inverters. It can be seen that the case 3 and the proposed approach (case 4) can achieve local active and reactive power supply of the microgrid loads. However, the full and partial absorption of reactive power in case 1 and case 2, respectively, resulting in decreasing the energy efficiency of the power system. This is due to the power losses in the transmission lines, which depend on the conductor properties and the distance between the load and the grid. Whereas, local partial reactive power supply in case 2 can reduce the transmission line losses. The proposed sharing approach in case 4 in addition to case 3 helps at eliminating the power loss that is related to the reactive power in the transmission lines. From another side, the local reactive power supply imposes additional stresses on the power electronic components of the SMES and PV inverters. For case 1, there are not added power losses in the inverter system, and hence no additional thermal stresses due to the lack of reactive power injection by the inverters. Whereas, the proposed approach and case 2 perform partial reactive power injection of each inverter (50% of load). This, in turn, results in additional power losses in the inverters according to the amount of the reactive power share. Case 3 represents the highest stress inverters due to the full reactive power compensation by the PV inverter. As a result, increased thermal stresses exist in case 3, which require more

TABLE 2. Performance indices comparison of the proposed strategy.

Performance index	Case 1	Case 2	Case 3	Case 4
Property	PV only without injecting reactive power (i.e., $Q_{pv} = 0.0$)	PV only with injecting reactive power is equal to 50% of the load reactive power (i.e., $Q_{pv} = 50\%Q_l$)	PV only with injecting reactive power is equal to full load reactive power (i.e., $Q_{pv} = 100\%Q_l$)	PV and SMES with equally sharing of the injecting load reactive power (i.e., $Q_{pv} = 50\%Q_l$ and $Q_{sm} = 50\%Q_l$)
Local active/reactive power supply	Not achieved	Not achieved	Not achieved	Achieved
Energy efficiency	Very low (the total required reactive power is absorbed from the grid with high transmission line power losses)	Low (half of the required reactive power is absorbed from the grid with high transmission line power losses)	Medium (average power losses of 2.457 kW for fixed load scenario and average power losses of 2.179 kW for variable load)	High (average power losses of 1.826 kW for fixed load scenario and average power losses of 1.696 kW for variable load)
Component stresses	Normal	Medium	Highest	Medium

cooling systems, higher ratings of power components, and reduce the operating lifetime of the inverters.

VI. CONCLUSION

This paper has presented an efficient reactive power sharing methodology between hybrid renewable energy generation and energy storage systems. The proposed method benefits the recent smart functionalities of PV and SMES power inverter at supporting the local load supply. In the proposed method, both of the PV and SMES inverters perform the DSTATCOM function. Therefore, the local reactive power supply can be achieved without transmission line losses and/or oversizing of the system components. The addition of the SMES helps at suppressing the fluctuations of the PV generation in addition to storing the excess PV energy for the night use. A microgrid with fixed and variable load scenarios are tested for the different operating modes. The results show that the proposed method can achieve optimized reactive power dispatch between the PV and SMES inverter. Moreover, the results of the tested case study show that the proposed reactive power sharing between the PV and SMES inverter achieves lower power losses than without sharing by 25.7% and 22.2% at fixed and variable load scenarios, respectively. The proposed reactive power sharing strategy preserves reduced thermal stresses due to the reduced power losses than without sharing. Therefore, a longer lifetime can be achieved for the grid integration inverters. The new proposed method offers a golden solution for achieving cleanliness environment, reducing the dependency on fossil fuel consumption, and comprehensive support of utility grid sustainability and reliability.

REFERENCES

[1] R. Tang, "Large-scale photovoltaic system on green ship and its MPPT controlling," *Sol. Energy*, vol. 157, pp. 614–628, Nov. 2017, doi: 10.1016/j.solener.2017.08.058.

[2] K. Mahmoud and M. Abdel-Nasser, "Fast yet accurate energy-loss-assessment approach for analyzing/sizing PV in distribution systems using machine learning," *IEEE Trans. Sustain. Energy*, vol. 10, no. 3, pp. 1025–1033, Jul. 2019, doi: 10.1109/tste.2018.2859036.

[3] S. M. Said, M. Aly, B. Hartmann, A. G. Alharbi, and E. M. Ahmed, "SMES-based fuzzy logic approach for enhancing the reliability of microgrids equipped with PV generators," *IEEE Access*, vol. 7, pp. 92059–92069, 2019, doi: 10.1109/access.2019.2927902.

[4] M. Aly, G. M. Dousoky, and M. Shoyama, "Design and validation of SVPWM algorithm for thermal protection of T-type three-level inverters," in *Proc. IEEE Int. Telecommun. Energy Conf. (INTELEC)*, Oct. 2015, pp. 1–6.

[5] K. M. Kotb, S. M. Said, A. Dan, and B. Hartmann, "Stability enhancement of isolated-microgrid applying solar power generation using SMES based FLC," in *Proc. 7th Int. Istanbul Smart Grids Cities Congr. Fair (ICSG)*, Apr. 2019, pp. 104–108.

[6] S. M. Said, E. A. Mohamed, and B. Hartmann, "Coordination strategy for digital frequency relays and energy storage in a low-inertia microgrid," *J. Power Technol.*, vol. 99, no. 4, pp. 254–263, 2020.

[7] J.-X. Jin and X.-Y. Chen, "Cooperative operation of superconducting fault-current-limiting cable and SMES system for grounding fault protection in a LVDC network," *IEEE Trans. Ind. Appl.*, vol. 51, no. 6, pp. 5410–5414, Dec. 2015, doi: 10.1109/tia.2015.2438252.

[8] S. Said, M. Aly, and B. Hartmann, "A robust SMES control for enhancing stability of distribution systems fed from intermittent wind power generation," *TURKISH J. Electr. Eng. Comput. Sci.*, vol. 27, no. 5, pp. 3883–3898, Sep. 2019.

[9] T. Penthia, A. K. Panda, and S. K. Sarangi, "Implementing dynamic evolution control approach for DC-link voltage regulation of superconducting magnetic energy storage system," *Int. J. Elect. Power Energy Syst.*, vol. 95, pp. 275–286, Feb. 2018, doi: 10.1016/j.ijepes.2017.08.022.

[10] M. Aly, E. M. Ahmed, and M. Shoyama, "An improved model predictive controller for highly reliable grid connected photovoltaic multilevel inverters," in *Proc. IEEE Int. Telecommun. Energy Conf. (INTELEC)*, Oct. 2017, pp. 450–455.

[11] A. Elmelegi, M. Aly, E. M. Ahmed, and A. G. Alharbi, "A simplified phase-shift PWM-based feedforward distributed MPPT method for grid-connected cascaded PV inverters," *Sol. Energy*, vol. 187, pp. 1–12, Jul. 2019, doi: 10.1016/j.solener.2019.05.021.

[12] E. M. Ahmed, M. Aly, A. Elmelegi, A. G. Alharbi, and Z. M. Ali, "Multifunctional distributed MPPT controller for 3P4W grid-connected PV systems in distribution network with unbalanced loads," *Energies*, vol. 12, no. 24, p. 4799, Dec. 2019, doi: 10.3390/en12244799.

[13] M. Aly, E. M. Ahmed, and M. Shoyama, "Thermal and reliability assessment for wind energy systems with DSTATCOM functionality in resilient microgrids," *IEEE Trans. Sustain. Energy*, vol. 8, no. 3, pp. 953–965, Jul. 2017, doi: 10.1109/tste.2016.2635200.

[14] I. Hussain, M. Kandpal, and B. Singh, "Grid integration of single stage SPV-STATCOM using cascaded 7-level VSC," *Int. J. Elect. Power Energy Syst.*, vol. 93, pp. 238–252, Dec. 2017, doi: 10.1016/j.ijepes.2017.06.005.

[15] M. Aly, E. M. Ahmed, and M. Shoyama, "Modulation method for improving reliability of multilevel T-type inverter in PV systems," *IEEE J. Emerg. Sel. Topics Power Electron.*, vol. 8, no. 2, pp. 1298–1309, Jun. 2020.

[16] B. Shaw, V. Mukherjee, and S. P. Ghoshal, "Solution of reactive power dispatch of power systems by an opposition-based gravitational search algorithm," *Int. J. Electr. Power Energy Syst.*, vol. 55, pp. 29–40, Feb. 2014, doi: 10.1016/j.ijepes.2013.08.010.

[17] A. A. Eladl and A. A. ElDesouky, "Optimal economic dispatch for multi heat-electric energy source power system," *Int. J. Electr. Power Energy Syst.*, vol. 110, pp. 21–35, Sep. 2019, doi: 10.1016/j.ijepes.2019.02.040.

[18] Z. Sahli, A. Hamouda, A. Bekrar, and D. Trentesaux, "Reactive power dispatch optimization with voltage profile improvement using an efficient hybrid algorithm," *Energies*, vol. 11, no. 8, p. 2134, Aug. 2018, doi: 10.3390/en11082134.

[19] L. Yuan, K. Meng, and Z. Y. Dong, "Hierarchical control scheme for coordinated reactive power regulation in clustered wind farms," *IET Renew. Power Gener.*, vol. 12, no. 10, pp. 1119–1126, Jul. 2018, doi: 10.1049/iet-rpg.2017.0835.

[20] R. Chilipi, N. Alsayari, and A. El Aroudi, "Coordinated control of parallel operated renewable-energy-based DG systems," *IET Renew. Power Gener.*, vol. 12, no. 14, pp. 1623–1632, Oct. 2018, doi: 10.1049/iet-rpg.2018.5287.

[21] K. Alboaouh and S. Mohagheghi, "Voltage and power optimization in a distribution network with high PV penetration," in *Proc. IEEE/PES Transmiss. Distrib. Conf. Expos. (T&D)*, Apr. 2018, pp. 1–9, doi: 10.1109/tdc.2018.8440384.

[22] P. Mukherjee and V. V. Rao, "Superconducting magnetic energy storage for stabilizing grid integrated with wind power generation systems," *J. Mod. Power Syst. Clean Energy*, vol. 7, no. 2, pp. 400–411, Oct. 2018, doi: 10.1007/s40565-018-0460-y.

[23] B. Singh, M. Kandpal, and I. Hussain, "Control of grid tied smart PV-DSTATCOM system using an adaptive technique," *IEEE Trans. Smart Grid*, vol. 9, no. 5, pp. 3986–3993, Sep. 2018, doi: 10.1109/tsg.2016.2645600.

[24] S. Sharouni and M. Hedayati, "Superconductor magnetic energy storage system usage for distributed generation: Active/reactive power and voltage controller design in connected and disconnected cases," *Int. Trans. Electr. Energy Syst.*, vol. 28, no. 5, p. e2531, Jan. 2018, doi: 10.1002/etep.2531.

[25] A. Azizi, P.-O. Logerais, A. Omeiri, A. Amiar, A. Charki, O. Riou, F. Delaleux, and J.-F. Durastanti, "Impact of the aging of a photovoltaic module on the performance of a grid-connected system," *Sol. Energy*, vol. 174, pp. 445–454, Nov. 2018, doi: 10.1016/j.solener.2018.09.022.

[26] F. Hans, W. Schumacher, and L. Harnefors, "Small-signal modeling of three-phase synchronous reference frame phase-locked loops," *IEEE Trans. Power Electron.*, vol. 33, no. 7, pp. 5556–5560, Jul. 2018, doi: 10.1109/tpel.2017.2783189.

[27] R. Teodorescu, M. Liserre, and P. Rodríguez, *Grid Converters for Photovoltaic and Wind Power Systems*. Hoboken, NJ, USA: Wiley, Jan. 2011, doi: 10.1002/9780470667057.

[28] S. M. Said, H. S. Salama, B. Hartmann, and I. Vokony, "A robust SMES controller strategy for mitigating power and voltage fluctuations of grid-connected hybrid PV–wind generation systems," *Electr. Eng.*, vol. 101, no. 3, pp. 1019–1032, Sep. 2019, doi: 10.1007/s00202-019-00848-z.

[29] Y. Deng, J. Li, K. H. Shin, T. Viitanen, M. Saeedifard, and R. G. Harley, "Improved modulation scheme for loss balancing of three-level active NPC converters," *IEEE Trans. Power Electron.*, vol. 32, no. 4, pp. 2521–2532, Apr. 2017, doi: 10.1109/tpel.2016.2573823.

[30] S. M. Said, A. Ali, and B. Hartmann, "Tie-line power flow control method for grid-connected microgrids with SMES based on optimization and fuzzy logic," *J. Mod. Power Syst. Clean Energy*, vol. 8, no. 5, pp. 941–950, 2020.

[31] S. M. Said, M. Aly, E. A. Mohamed, and B. Hartmann, "Analysis and comparison of SMES device power losses considering various load conditions," in *Proc. IEEE Conf. Power Electron. Renew. Energy (CPERE)*, Oct. 2019, pp. 1–5, doi: 10.1109/cpere45374.2019.8980205.

SAYED M. SAID was born in Aswan, Egypt. He received the B.Sc. and M.Sc. degrees in electrical engineering from Aswan University, in 2006 and 2014, respectively. He is currently pursuing the Ph.D. degree with the Faculty of Electrical Engineering and Informatics, Doctoral School of Electrical Engineering, Budapest University of Technology and Economics, Budapest, Hungary. Since 2010, he has been working as a Research Assistant with the Electrical Engineering Department. His research interests include power system analysis, renewable energies, power system control, wind energy with superconducting magnetic energy storage (SMES), and integration of wind/PV-based on SMES to the utility grids.

MOKHTAR ALY (Member, IEEE) received the B.Sc. and M.Sc. degrees in electrical engineering from Aswan University, Aswan, Egypt, in 2007 and 2012, respectively, and the Ph.D. degree from the Department of Electrical Engineering, Faculty of Information Science and Electrical Engineering, Kyushu University, Japan, in 2017.

He joined the Department of Electrical Engineering, Aswan University, as an Assistant Lecturer, in 2008, where he has been as an Assistant Professor with the Faculty of Engineering, since 2017. He is currently a Postdoctoral Researcher with the Solar Energy Research Center (SERC-Chile), Universidad Técnica Federico Santa María, Chile. His current research interests include reliability of power electronics systems especially in renewable energy applications, multi-level inverters, fault tolerant control, electric vehicles, and light emitting diode (LED) lamp drivers. He is a member of the IEEE Power Electronics Society (PELS), the IEEE Industrial Electronics Society (IES), and the IEEE Power and Energy Society (PES).
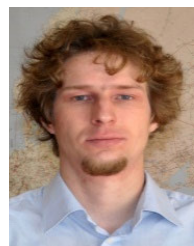
HARTMANN BALINT (Member, IEEE) received the M.Sc. degree in electrical engineering and the Ph.D. degree from the Budapest University of Technology and Economics (BME), in 2008 and 2013, respectively. He is currently an Associate Professor with the Department of Electric Power Engineering, BME, where he has supervised over 40 bachelor's and master's theses. He is also a Research Fellow with the Centre for Energy Research. He is also a Supervisor of four Ph.D. Students. His research interests include the role of energy storage in the power systems, computer modeling and simulation of distribution networks, and integration of variable renewable energy sources. From 2013 to 2019, he was a Board Member of the Hungarian Electrotechnical Association. He is the Chair of the IEEE PES Hungary Chapter.

• • •